ISSN 1674-1056
http://cpb.iphy.ac.cn
http://iopscience.iop.org/cpb
中国物理 B
Chinese Physics
中国物理
Chinese Physics B

Temperature effects on atmospheric continuous-variable quantum key distribution

Shu-Jing Zhang(张淑静), Hong-Xin Ma(马鸿鑫), Xiang Wang(汪翔), Chun Zhou(周淳), Wan-Su Bao(鲍皖苏), Hai-Long Zhang(张海龙)

Citation: Chin. Phys. B . 2019, 28(8): 080304. **doi:** 10.1088/1674-1056/28/8/080304
Journal homepage: http://cpb.iphy.ac.cn; http://iopscience.iop.org/cpb

What follows is a list of articles you may be interested in

Research on co-propagation of QKD and classical communication by reducing the classical optical power

Ru-Shi He(何如适), Mu-Sheng Jiang(江木生), Yang Wang(汪洋), Ya-Hui Gan(甘亚辉), Chun Zhou(周淳), Wan-Su Bao(鲍皖苏)

Chin. Phys. B . 2019, 28(4): 040303. **doi:** 10.1088/1674-1056/28/4/040303

Noiseless linear amplification for the single-photon entanglement of arbitrary polarization-time-bin qudit

Ling-Quan Chen(陈灵泉), Yu-Bo Sheng(盛宇波), Lan Zhou(周澜)

Chin. Phys. B . 2019, 28(1): 010302. **doi:** 10.1088/1674-1056/28/1/010302

Direct measurement of the concurrence of hybrid entangled state based on parity check measurements

Man Zhang(张曼), Lan Zhou(周澜), Wei Zhong(钟伟), Yu-Bo Sheng(盛宇波)

Chin. Phys. B . 2019, 28(1): 010301. **doi:** 10.1088/1674-1056/28/1/010301

Security of a practical semi-device-independent quantum key distribution protocol against collective attacks

Wang Yang, Bao Wan-Su, Li Hong-Wei, Zhou Chun, Li Yuan

Chin. Phys. B . 2014, 23(8): 080303. **doi:** 10.1088/1674-1056/23/8/080303

Entangled quantum heat engine based on two-qubit Heisenberg *XY* model

He Ji-Zhou,He Xian,Zheng Jie

Chin. Phys. B . 2012, 21(5): 050303. **doi:** 10.1088/1674-1056/21/5/050303

Temperature effects on atmospheric continuous-variable quantum key distribution*

Shu-Jing Zhang(张淑静), Hong-Xin Ma(马鸿鑫), Xiang Wang(汪翔), Chun Zhou(周淳), Wan-Su Bao(鲍皖苏), and Hai-Long Zhang(张海龙)†

Henan Key Laboratory of Quantum Information and Cryptography, Zhengzhou Information Science and Technology Institute, Zhengzhou 450001, *China*

(Received 2 February 2019; revised manuscript received 20 May 2019; published online 9 July 2019)

Compared with the fiber channel, the atmospheric channel offers the possibility of a broader geographical coverage and more flexible transmission for continuous-variable quantum key distribution (CVQKD). However, the fluctuation of atmospheric conditions will lead to the loss of performance in atmospheric quantum communication. In this paper, we study how temperature affects atmospheric CVQKD. We mainly consider the temperature effects on the transmittance and interruption probability. From the numerical simulation analysis, it can be shown that the performance of atmospheric CVQKD is improved as temperature increases, with the other factors fixed. Moreover, the results in this work can be used to evaluate the feasibility of the experimental implementation of the atmospheric CVQKD protocols.

Keywords: atmospheric continuous-variable quantum key distribution, temperature effects, performance, secret key rate

PACS: 03.67.Dd, 03.67.Hk, 03.67.–a **DOI:** 10.1088/1674-1056/28/8/080304

1. Introduction

Quantum key distribution (QKD),[1,2] which allows two legitimate parties to establish a random secret key between them, is probably the most significant branch of quantum communication. The security of QKD is provided by the laws of quantum mechanics. Compared with the discrete-variable quantum key distribution (DVQKD) system,[3] the CVQKD system has the following advantages: first, the preparation of light sources are relatively simple; second, the detectors have low cost and high detection efficiency; and finally, it can be effectively compatible with existing optical communication systems. For these reasons, the CVQKD has received extensive attention and be studied in depth in the area of quantum communication.[4]

The quantum channel is one of essential factors in the QKD systems. The most common channel in implementation is the optical fiber and the free space channel,[5,6] and the latter provides great flexibility in the establishment of infrastructure and in the connection with moving objects.[7,8] However, the negative effects of the free-space channel in atmosphere such as the background light and atmospheric turbulence cannot be ignored.[9] Therefore, it is necessary to establish a comprehensive transmission model and carry out the corresponding performance analysis of QKD in the atmosphere. The model was studied in the recent years.[10–14] An elliptical beam model considering beam wandering, broadening and deformation has been established for quantum light through the atmospheric channel,[15] then others factors, such as arrival time fluctuations and angle-of-arrival fluctuations, were also considered in this model.[16–19] However, in the QKD system, the quantum states in atmospheric channels are sensitive to fluctuation of temperature. When the beam propagates in the turbulent atmosphere, the temperature fluctuation of the turbulent atmosphere causes the refractive index to fluctuate,[20] which leads to a series of turbulence effects such as beam wandering, scintillation, transmission fluctuation, communication interruption, etc. Therefore, the temperature effects should be considered in the atmospheric CVQKD.[21–26]

In this paper, we mainly consider the temperature effects on atmospheric CVQKD, through taking into consideration two parameters that can affect the secret key rate. First, considering the temperature effects on transmittance, our results demonstrate that the temporal pulse broadening decreases with the increase of temperature. Second, our results demonstrate that the interruption probability decreases with the increase of temperature. Finally, the performance of secret key rate is analyzed with the temperature fluctuation. It is shown that secret key rate coincides positively with temperature fluctuation. Hence, the studies could contribute to evaluating the feasibility and performance of atmospheric CVQKD protocols.

2. Temperature effects on atmospheric CVQKD

Atmospheric CVQKD indicates that the parameters of protocol are closely related to atmospheric effect. The atmospheric channel plays a vital role in affecting the performance of the atmospheric CVQKD protocol. The effects of atmospheric channel on the performance of temporal pulse broadening are divided into two types: the first is atmospheric scat-

*Project supported by the National Natural Science Foundation of China (Grant No. 61505261).

†Corresponding author. E-mail: zhhl049@126.com

© 2019 Chinese Physical Society and IOP Publishing Ltd

tering and the second is atmospheric turbulence. In this paper, only the effect of atmospheric turbulence is addressed at great length.

2.1. Effect of temperature on transmittance

The effect of atmospheric turbulence on the atmospheric transmission of beam pulses is actually caused by the random fluctuation of atmospheric refractive index on a spatial scale. The different variance of atmospheric refractive index fluctuation represents different turbulence intensity. Because refractive index is a function of temperature in atmosphere, the properties of refractive field are closely related to the properties of temperature field. The temporal pulse broadening of atmospheric means the diffusion of pulse energy in temporal domain. In the practical experiment, signal detection is conducted in high speed sampling in temporal domain, and the maximum value is selected as the detection result, which means that the temporal pulse broadening introduces an equal transmittance. As shown in Fig. 1,[21] the temporal width of both LO and signal pulse are broadened after passing through the atmospheric channel.



Fig. 1. Temporal pulse broadening. After signal and LO pulse pass through atmosphere, they broaden.

We can evaluate the mean value of transmittance for equality via approximately calculating the intensity of free space irradiation of collimated beams under near and far field. The transmittance introduced by mean value of pulse broadening can be expressed as[27–29]

$$T_{\text{bro}} = \frac{T_0}{T_1}, \tag{1}$$

where T_0 is the initial pulse half-width and T_1 is described as

$$T_1 = \sqrt{T_0^2 + 8a_1}, \tag{2}$$

where T_1 is the estimation of the broadened half-width at receiver, and $a_1 = 0.39C_n^2 L L_0^{5/3} c^{-2}$, with C_n^2 being the index of refraction structure parameter.

Because of the randomness, irregularity, and temporal and spatial limitation of turbulence, it is difficult to directly measure the turbulence intensity. The refractive index structure parameter describes the strength of the atmospheric refractive index, which can be used to represent the strength of turbulence. According to the structure function of Tatarskii, the refractive index structure function C_n^2 of near-surface atmospheric turbulence can be written as[20]

$$C_n^2 = \left(79 \times 10^{-6} \frac{P_{\text{pre}}}{T_{\text{t}}^2}\right)^2 C_{\text{T}}^2, \tag{3}$$

where P_{pre} is the atmospheric pressure, T_{t} is the temperature, and C_{T}^2 is the index of temperature structure parameter.

We consider pulse broadening rate, and define the pulse broadening rate as[21]

$$TR = \frac{T_1 - T_0}{T_0}. \tag{4}$$

Figure 2(a) shows that the equivalent transmittance varies with temperature and initial pulse half-width. Figure 2(b) shows the tendency of equivalent transmittance with temperature for different initial pulse half-widths. At the same temperature, the larger the half-width of the initial pulse, the greater the transmittance will be; and the higher the temperature, the higher the transmittance will be. The effects of distance and temperature on transmittance can also be estimated and results are shown in Fig. 2(c), where the initial pulse half-width is shown. It can be seen that any increase in temperature or decrease in distance will lead to an increase in transmission.

The results of the relationship among initial pulse half-width, temperature and broadening rate are given in Fig. 3(a). Figure 3(b) shows the relation between the broadening rate and temperature under different half-widths of initial pulse. The higher the temperature, the smaller the broadening rate is. Figure 3(c) shows that the temporal pulse broadening rate varies with temperature and distance. It is apparent that the temporal pulse broadening rate increases with the decrease of temperature and the increase of distance.

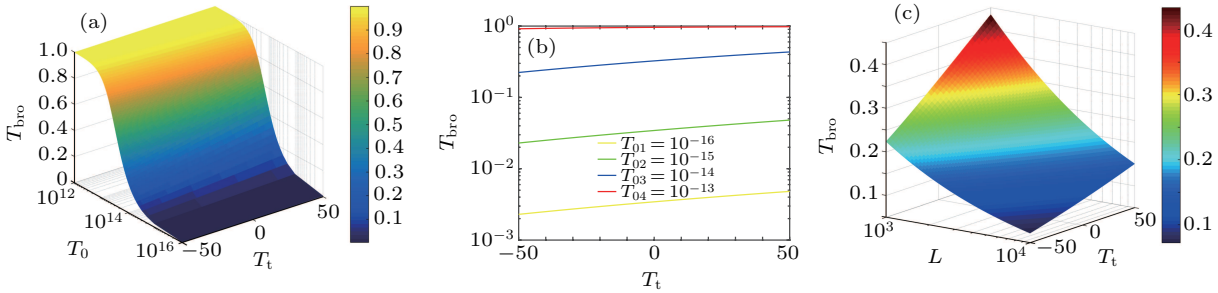


Fig. 2. (a) Variation of mean value of pulse broadening with temperature and initial pulse half-width, where $C_{\text{T}}^2 = 0.001$ and $L_0 = 0.4$ m. (b) Changes of equivalent transmittance with temperature for initial pulse half-widths of 10^{-16}, 10^{-15}, 10^{-14}, 10^{-13} respectively. (c) Transmittance varying with distance and temperature when initial pulse half-width is 10^{-14}.

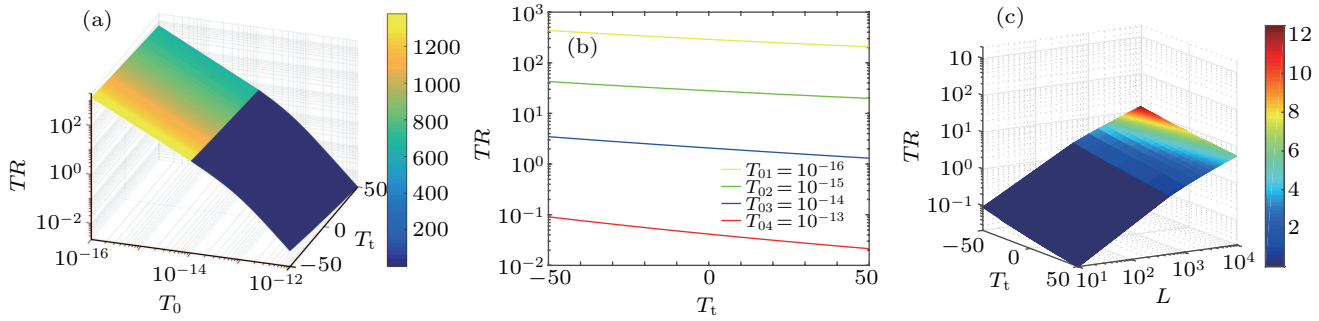


Fig. 3. (a) Pulse broadening rate varying with temperature and initial pulse half-width, (b) tendency of the broadening rate with respect to temperature for half-widths of initial pulse of 10^{-16}, 10^{-15}, 10^{-14}, 10^{-13}. (c) Pulse broadening rate *versus* temperature and distance for initial pulse half-width of 10^{-14}.

From this analysis it can be seen that the temporal pulse broadening rate and the transmittance varying with temperature and distance can be acquired, which provides a judgment basis for the improvement of performing QKD. When implemented with other parameters, the protocol performance can be greatly improved by selecting appropriate parameters on the basis of the relationship among temperature, temporal pulse broadening and transmittance.

2.2. Effect of temperature on interruption probability

In the case of atmospheric turbulence, due to the variation of refractive index, the beam angle-of-arrival will fluctuate, which makes the communication interrupted possibly. It can be seen from the previous analysis that the refractive index corresponds to temperature fluctuation, thus the relationship between temperature and interruption probability is under consideration in this subsection.[30,31]

First, the fluctuation of angle-of- arrival is analyzed. As shown in Fig. 4,[16] after being propagated through the atmosphere, the beam randomly jitters in the plane of the receiving telescope due to turbulence.

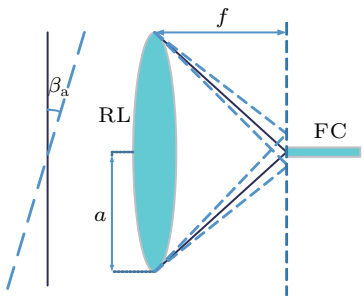


Fig. 4. Communication interruption caused by beam fluctuations on the receiving plane. β_a: angle-of-arrival, RL: receiving lens, FC: fiber core.

At first, we assume that the mean value of arriving angle is[21]

$$\langle \beta_a^2 \rangle = \frac{\langle \Delta x^2 \rangle}{L^2}. \tag{5}$$

In turbulence,

$$\langle \Delta x^2 \rangle = 0.33 W_0^2 \sigma_1^2 \Omega^{-7/6}, \quad \sigma_1^2 = 1.23 C_n^2 k^{7/6} L^{11/6},$$

and $k = 2\pi/\lambda$ is the optical wave number, λ is the wavelength, L is the propagation distance, W_0 is the transmitting lens radius, and $\Omega = kW_0^2/2L$ is the Fresnel parameter.

The interruption probability of communication can be shown as[21]

$$p = 1 - \int_{-0.5d_{\rm cor}}^{0.5d_{\rm cor}} \frac{1}{\sqrt{2\pi \langle \beta_a^2 \rangle} f} \exp\left(\frac{-l^2}{2f^2 \langle \beta_a^2 \rangle} \right) {\rm d}l, \tag{6}$$

where $d_{\rm cor}$, l, and f are, respectively, the diameter of the fiber core, the focal length of receiving lens, and the distance between the center of fiber core and beam in fiber core plane. Combining Eq. (3) and Eq. (6), we can obtain the relationship between interruption probability and temperature. The effects of temperature on interrupt probability at four different distances, *i.e.*, 1000, 1500, 3000, 5000 m are shown in Fig. 5, from which it is obvious that for each distance, the interrupt probability tends to decrease with temperature increasing. As the distance increases, the interruption probability correspondingly increases. The parameters W_0, f, and λ are assigned to 80 mm, 220 mm, and 1550 nm, respectively.

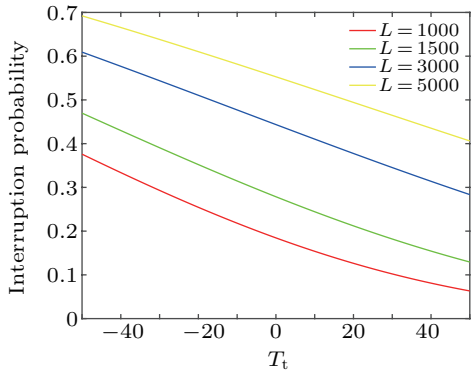


Fig. 5. Interruption probability varying with temperature at $W_0 =$ 80 mm, $f = 220$ mm, $\lambda = 1550$ nm, and $L = 1000$ m, 1500 m, 3000 m, 5000 m, respectively.

3. Secret key rate of atmospheric CVQKD

Next, the secret key rate of atmospheric CVQKD through fluctuating channel is analyzed. An atmospheric CVQKD protocol is shown in Fig. 6. The Einstein–Podolsky–Rosen (EPR) source generates an entangled state with variance V. The B_0 is a mode of the entangled state that is transmitted to Bob

through a fading channel that is depicted by a distribution of transmittance T, and Bob performs the heterodyne detection to measure the quadrature. The detection efficiency η is used to depict the imperfection of the detector and the electronic noise $v_{\rm el}$ contained in variance v.[21]

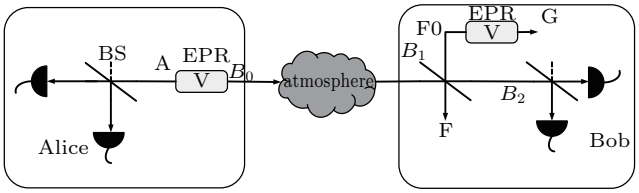


Fig. 6. CVQKD through atmospheric channel. BS: beam splitter.

The secret key rate K is given as[21]

$$K = \beta I_{\rm AB} - \chi_{\rm BE}. \tag{7}$$

When we take communication interruption probability into account in the secret key rate, the expression can be rewritten as[22]

$$K = (1-P)(\beta I_{\rm AB} - \chi_{\rm BE}), \tag{8}$$

where P is interruption probability, β is the reconciliation efficiency, $I_{\rm AB}$ is the Shannon mutual information of Alice and Bob, and $\chi_{\rm BE}$ is the Holevo quantity, which can be expressed as[23]

$$\chi_{\rm BE} = S(\rho_{\rm E}) - \int {\rm d}m_{\rm B}\, p(m_{\rm B}) S(\rho_{\rm E}^{m_{\rm B}}), \tag{9}$$

where $m_{\rm B}$ represents the measurement of Bob, $p(m_{\rm B})$ the probability density of the measurement, $\rho_{\rm E}^{m_{\rm B}}$ the eavesdropper's state conditional on Bob's measurement result, and $S(\cdot)$ the Von Neumann entropy.

Then, we should calculate $I_{\rm AB}$ and$\chi_{\rm BE}$ in order to obtain the secret key rate. The practical form of the two-mode squeezed state can be written as[24]

$$\gamma_{\rm AB} = \begin{pmatrix} VII & \sqrt{V^2-1}Z \\ \sqrt{V^2-1}Z & VII \end{pmatrix}, \tag{10}$$

where V represents Alice's modulation variance, $Z = {\rm diag}(1,-1)$, and $II = {\rm diag}(1,1)$.

On the assumption that the state is described by distribution of probabilities of transmittance $\{T_i\}$ through a fluctuating channel, and that we can use the mean value of transmittance $\langle T\rangle$ and the root mean square of transmittance $\langle\sqrt{T}\rangle$ to replace the fluctuating transmittance,[25] the covariance matrix can be expressed as

$$\gamma_{\rm AB} = \begin{pmatrix} VII & \langle\sqrt{T}\rangle\sqrt{V^2-1}Z \\ \langle\sqrt{T}\rangle\sqrt{V^2-1}Z & \langle T\rangle(V+1/\langle T\rangle - 1+\varepsilon)II \end{pmatrix}. \tag{11}$$

Now, the mutual information can be expressed as

$$I_{\rm AB} = \log_2 \frac{1}{1-\left[\langle\sqrt{T}\rangle^2 (V-1)/\langle T\rangle (V+\chi)\right]}, \tag{12}$$

where $\chi = 2(1+v_{\rm el})/\eta\langle T\rangle - 1 + \varepsilon$. And $\chi_{\rm BE}$ can also be obtained to be[32]

$$\chi_{\rm BE} = \sum_{i=1}^{2} G\left(\frac{\lambda_i - 1}{2}\right) - \sum_{i=3}^{5} G\left(\frac{\lambda_i - 1}{2}\right), \tag{13}$$

where $G(x) = (x+1)\log_2(x+1) - x\log_2(x)$.

4. Performance analysis

In this section, the final secret key rate in conjunction with the results from previous analyses is investigated. Here we do not consider the excess noise that changes with temperature, but we still examine the performance under different fixed excess noise levels, namely $\varepsilon = 0.01$, $\varepsilon = 0.03$, and $\varepsilon = 0.05$ in SNU.

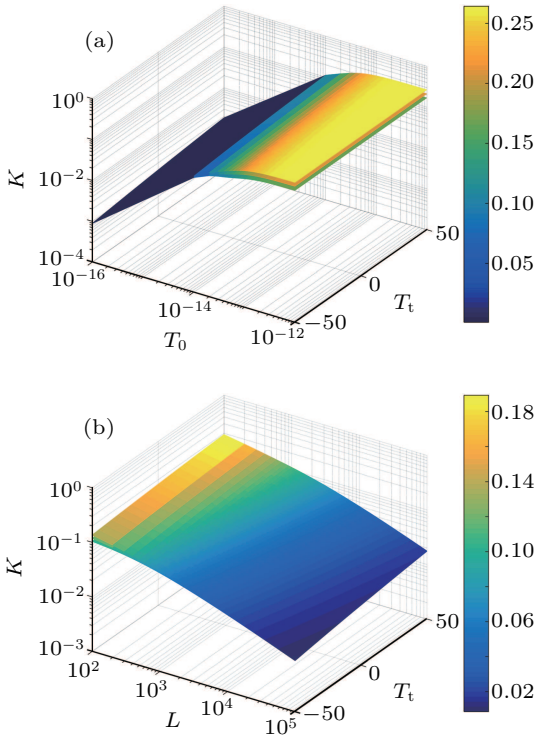


Fig. 7. (a) Secret key rate varying with initial pulse half-width and temperature at distance 1000 m. (b) Secret key rate varying with distance and temperature at initial pulse half-width.

First, in the analysis of the secret key rate, we consider only the effect of pulse broadening. As can be seen in Fig. 7(a), the secret key rate is higher where the initial pulse half-width is larger and the temperature is higher, because with the increase of the initial pulse half-width, the pulse is close to the classical optical communication, the pulse fluctuation caused by turbulence is smaller. In this figure, from top to bottom, the excess noise is $\varepsilon = 0.01$, $\varepsilon = 0.03$, and $\varepsilon = 0.05$, respectively. As we can see, the secret key rate decreases, but not much, as the excess noise increases. Figure 7(b) shows that with the increase of distance the secret key rate declines. In this figure, from top to bottom, the excess noise is $\varepsilon = 0.01$,

$\varepsilon = 0.03$, and $\varepsilon = 0.05$, respectively. This is the same as that in Fig. 7(a), and the effect of excess noise on secret key rate is not obvious.

Second, we take the interruption probability into consideration in the analysis of the secret key rate under diverse excess noise levels of $\varepsilon = 0.01$, $\varepsilon = 0.03$, and $\varepsilon = 0.05$. At the distance of 1500 m, the transmittance is 0.9. In Fig. 8, the secret key rate obviously decreases with the increase of interrupt probability. Since the increase of interruption probability means that the probability of successfully implementing CVQKD protocol decreases, which will lead to the decrease of secret key rate. Furthermore, smaller excess noise can achieve larger secret key rate. However, the change of excess noise does not affect the trend of curve that depicts the relationship between temperature and protocol performance.

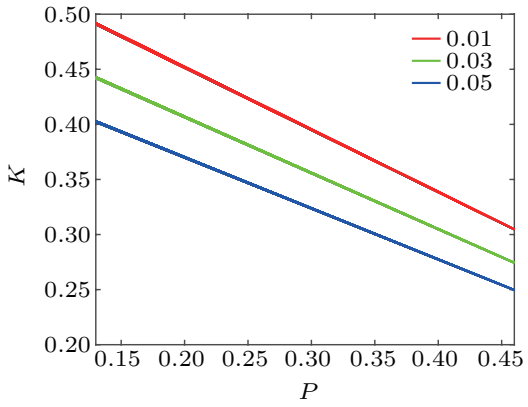


Fig. 8. Plots of secret key rate *versus* interruption probability.

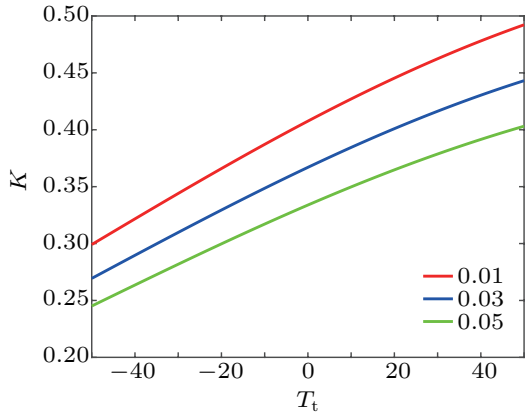


Fig. 9. Plots of secret key rate *versus* temperature, with considering all the effects of temperature studied in this paper.

Finally, this analysis is comprehensively combined to analyze the final secret key rate. We estimate the secret key rate in Eq. (8), where the effects of temperature on transmittance and interruption probability are both considered. As indicated in Fig. 9, the secret key rate is higher where the temperature is higher. Besides, the decrease of the excess noise level also increases the secret key rate. However, as the temperature increases, the secret key rate does not increase too much, which is not surprising. Indeed, when the CVQKD protocol is implemented in the atmospheric channel, due to turbulence regardless of the influence of temperature, the secret key rate is relatively small. Therefore, when adding the temperature effect into the estimation of secret key rate fluctuation, the variable quantity of secret key rate is small. With the development of atmospheric channel CVQKD system, the secret key rate must be improved. In this case, the fluctuation of temperature will cause large variable quantity of secret key rate. Hence, considering the effects of temperature on secret key rate is important not only for current research but is also potentially important for future atmospheric channel implementation of CVQKD protocols.

5. Conclusions and perspectives

In this paper, we perform an analysis of atmospheric CVQKD with the temperature effect and estimate its performance. It can be seen from the analysis that the temporal pulse broadening varies with atmospheric temperature, and the smaller the initial pulse half-width, the larger the temporal pulse broadening is, which means that in the practical application, the communication parties can choose different initial pulse half-widths according to the actual temperature to achieve the minimum temporal pulse broadening. Furthermore, we study the effect of temperature on communication interruption, and the probability of communication interruption increases with the decrease of temperature. That is to say, when we implement an atmospheric CVQKD, and consider the effect of temperature on interruption probability, we can choose a relatively high temperature to reduce the probability of interruption. We assess the secret key rate with temperature effect, initial pulse half-width and distance. According to our analysis, the increase of temperature or the decline of distance will lead the secret key rate to increase. In general, the results can conduce to the performance assessment of practical atmospheric CVQKD. However, atmospheric turbulence is exceedingly complex. Other parameters that describe atmospheric turbulence also have an influence on turbulence, which in turn affects the atmospheric CVQKD. Therefore, other factors, such as pressure, humidity and wind speed, should be taken into account in further studies.

References

[1] Bennett C H, Brassard G, Popescu S, *et al.* 1996 *Phys. Rev. Lett.* **76** 722
[2] Ma H X, Bao W S and Li H W 2016 *Chin. Phys. B* **25** 080309
[3] Huang D, Fang J and Zeng G H 2013 *Chin. Phys. Lett.* **30** 114209
[4] Guo Y, Su Y, Zhou J, Zhang L and Huang D 2019 *Chin. Phys. B* **28** 010305
[5] Yan X, Zhang P F, Zhang J H, Qiao C H and Fan C Y 2016 *Chin. Phys. B* **25** 084204

[6] Dixon A R, Yuan Z L, Dynes J F, *et al.* 2008 *Opt. Express* **16** 18790
[7] Nauerth S, Moll F, Fuchs C, *et al.* 2013 *Nat. Photon.* **7** 382
[8] Zhang S L, Jin C H, Guo G C, *et al.* 2017 *Chin. Phys. Lett.* **34** 040302
[9] Wang L G, Wu Z S, Wang M J, Cao Y H and Zhang G 2014 *Chin. Phys. B* **23** 094202
[10] Ma J, Fu Y L, Yu S Y, Xie X L and Tan L Y 2018 *Chin. Phys. B* **27** 034201
[11] Heim B, Peuntinger C, Killoran N, *et al.* 2014 *New J. Phys.* **16** 113018
[12] Ma E L, Han Z F, Gao S S, *et al.* 2005 *New J. Phys.* **7** 215
[13] Semenov A A, Vogel W 2009 *Phys. Rev. A* **80** 021802
[14] Usenko V C, Heim B, Peuntinger C, *et al.* 2012 *New J. Phys.* **14** 093048
[15] Vasylyev D, Semenov A A, Vogel W, *et al.* 2016 *Phys. Rev. Lett.* **117** 090501
[16] Wang Y J, Fan C Y, Wei H L, *et al.* 2015 *Laser Beam Propagation and Applications through the Atmosphere and Sea Water* (Beijing: National Defense Industry Press)
[17] Vasylyev D, Semenov A A, Vogel W, *et al.* 2017 *Phys. Rev. A* **96** 043856
[18] Andrews L C, Phillips R L and Hopen C Y 2001 *Laser Beam Scintillation with Applications* (Bellingham, WA: SPIE)
[19] Guo Y, Xie C L, Huang D, *et al.* 2017 *Phys. Rev. A* **96** 022320
[20] Tatarskii V I 1978 *Wave Propagation in Turbulent Medium* (Beijing: Science press)
[21] Wang S Y, Huang P and Zeng G H 2018 *New J. Phys.* **20** 083037
[22] Kraus B, Gisin N, Renner R, *et al.* 2005 *Phys. Rev. Lett.* **95** 080501
[23] Holevo A S 1973 *Probl Peredachi Inf.* **9** 3
[24] Diamanti E and Leverrier A 2015 *Entropy* **17** 6072
[25] Dong R, Lassen M, Andersen U L, *et al.* 2010 *Phys. Rev. A* **82** 012312
[26] Guo Y, Xie C L, Zeng G H, *et al.* 2018 *Phys. Rev. A* **97** 052326
[27] Ziolkowski R W and Judkins J B 1992 *J. Opt. Soc. Am. A* **9** 2021
[28] Young C Y, Andrews L C, Ishimaru A, *et al.* 1998 *Appl. Opt.* **37** 7655
[29] Kelly D and Andrews L C 1999 *Waves Random Media* **9** 307
[30] Andrews L C and Phillips R L 2005 *Laser Beam Propagation Through Random Media* (Bellingham WA: SPIE press)
[31] Song Z F, *et al.* 1990 *Applied Atmospheric Optics.* (Beijing: China Meteorological Press)
[32] Guo H, Li Z Y, Peng X, *et al.* 2016 *Quantum Cryptography* (Beijing: National Defense Industry Press)